Journal of Engineering Physics and Thermophysics, Vol. 82, No. 5, 2009

CONJUGATE MIXED CONVECTION UNDER MASS-TRANSFER CONDITIONS

G. V. Kuznetsov[a] **and M. A. Sheremet**[b]

UDC 669.86:536.21

Mathematical modeling of the conjugate mixed convection in a rectangular region in the presence of heat- and mass-release sources has been carried out. The distributions of thermohydrodynamic and diffusion parameters, which characterize the basic regularities of the process under study, have been obtained. The influence of the nonstationarity factor and of the intensity of heat-release and mass-release sources on the formation and development of both vortex hydrodynamic structures and temperature fields has been investigated. The distributions of local characteristics (streamlines, isotherms) and integral characteristics (average Nusselt and Sherwood numbers) have been obtained.

Keywords: *conjugate heat transfer, mixed convection, mass transfer, numerical analysis, local heat- and mass-release sources.*

Introduction. Considerable recent attention has been given to an analysis of the mechanisms of convective heat and mass transfer in closed regions (enclosures) filled with both liquid and porous material [1–5]. The processes of combined convective heat and mass transfer are characteristic of problems of many sciences: oceanography, astrophysics, geology, chemistry, and others [6–8]. It has been established [9, 10] that allowance for the influence of heat-accumulating external walls is required in analyzing convective heat and mass transfer in enclosures.

Many processes of convective heat transfer are realized in nature and technology in combination with the processes of mass transfer of components whose content (e.g., by weight) is low but the effect of presence can be large-scale [8, 11]. However, despite a rather active recent study of mixed-convection processes [1, 12–14], mass transfer occurring in combination with them in regions with walls of finite thickness remains to be investigated.

The present work seeks to numerically analyze nonstationary mixed convection in a rectangular region with walls of finite thickness in the presence of local heat- and mass-release sources under the conditions of convective-radiative heat exchange with the external medium.

Mathematical Model. We consider a boundary-value problem of nonstationary conjugate heat and mass transfer in a rectangular region (Fig. 1). The solution domain includes both the walls of finite dimensions and a gas cavity with heat and impurity sources. Gas 8 containing a certain impurity of prescribed initial concentration is supplied to the cavity. The gas escapes via outlet 9. In the inlet zone, there is a local mass source 7 the concentration of the second component in which remains constant throughout the process, as does the temperature on the heat-release source. The horizontal walls ($y = 0$, $y = L_y$) and the vertical wall ($x = L_x$) forming the gas cavity are assumed to be heat-insulated on the outside. Convective-radiative heat exchange with the environment is carried out at the boundary $x = 0$.

It is assumed that the thermophysical properties of the wall and gas material are temperature-independent, whereas the flow regime is laminar. The gas is considered to be a viscous heat-conducting Newtonian fluid satisfying the Boussinesq approximation. We take that the gas motion and heat transfer in the internal volume are planar, heat exchange by radiation from the heat-release source and between the walls is negligible compared to convective heat exchange, and the gas is absolutely transparent to thermal radiation. It is assumed that terms in the energy equation that characterize viscous dissipation and work of pressure are negligible. The effects of second order (diffusion thermal effect and thermal diffusion) are disregarded, too.

In such a statement, the process of transfer of heat and mass in the region in question (Fig. 1) is described by the system of unsteady two-dimensional convection equation in the Boussinesq approximation [6–8, 11] and the dif-

[a]Tomsk Polytechnic University, 30 Lenin Ave., Tomsk, 634050, Russia; [b]Tomsk State University, 36 Lenin Ave., Tomsk, 634050, Russia; email: Michael-sher@yandex.ru. Translated from Inzhenerno-Fizicheskii Zhurnal, Vol. 82, No. 5, pp. 886–895, September–October, 2009. Original article submitted July 22, 2008.

 1062-0125/09/8205-0890

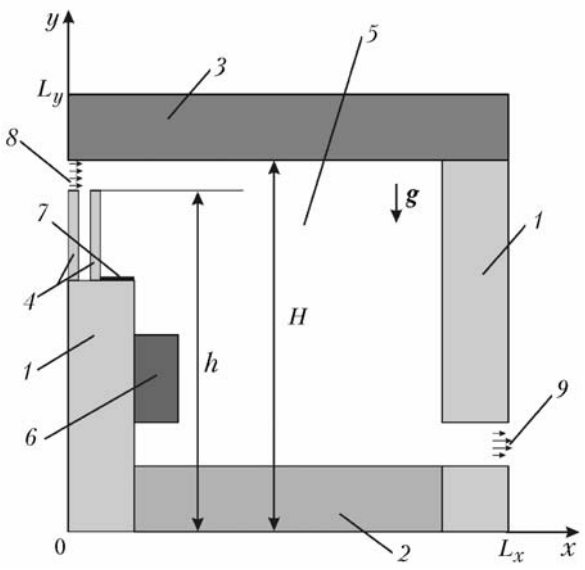

Fig. 1. Solution domain of the problem in question: 1, 2, 3, and 4) solid walls; 5) gas cavity; 6) heat-release source; 7) mass-release source; 8) inlet; 9) outlet.

fusion equation [1, 8] in the gas cavity and by the unsteady heat-conduction equation for solid-material elements [15] with nonlinear boundary conditions.

A mathematical model is formulated in the dimensionless variables stream function–vorticity vector–temperature–concentration. The length of the considered solution domain along the x axis is selected as the distance scale. To reduce the system of equations to dimensionless form we use the following relations:

$$X=\frac{x}{L_x},\quad Y=\frac{y}{L_x},\quad \tau=\frac{t}{t_0},\quad U=\frac{u}{V_{\text{in}}},\quad V=\frac{v}{V_{\text{in}}},\quad \Theta=\frac{T-T_0}{T_{\text{h.s}}-T_0},\quad \xi=\frac{C-C_0}{C_{\text{c.s}}-C_0},\quad \Psi=\frac{\psi}{\psi_0},\quad \Omega=\frac{\omega}{\omega_0}.$$

The dimensionless equations of conjugate heat and mass transfer are as follows:

for the gas (5 in Fig. 1)

$$\frac{\partial\Omega}{\partial\tau}+\frac{\partial\Psi}{\partial Y}\frac{\partial\Omega}{\partial X}-\frac{\partial\Psi}{\partial X}\frac{\partial\Omega}{\partial Y}=\frac{1}{\text{Re}}\left(\frac{\partial^2\Omega}{\partial X^2}+\frac{\partial^2\Omega}{\partial Y^2}\right)+\frac{\text{Gr}}{\text{Re}^2}\left(\frac{\partial\Theta}{\partial X}+\text{Br}\frac{\partial\xi}{\partial X}\right), \tag{1}$$

$$\frac{\partial^2\Psi}{\partial X^2}+\frac{\partial^2\Psi}{\partial Y^2}=-\Omega, \tag{2}$$

$$\frac{\partial\Theta}{\partial\tau}+\frac{\partial\Psi}{\partial Y}\frac{\partial\Theta}{\partial X}-\frac{\partial\Psi}{\partial X}\frac{\partial\Theta}{\partial Y}=\frac{1}{\text{Re}\,\text{Pr}}\left(\frac{\partial^2\Theta}{\partial X^2}+\frac{\partial^2\Theta}{\partial Y^2}\right), \tag{3}$$

$$\frac{\partial\xi}{\partial\tau}+\frac{\partial\Psi}{\partial Y}\frac{\partial\xi}{\partial X}-\frac{\partial\Psi}{\partial X}\frac{\partial\xi}{\partial Y}=\frac{1}{\text{Re}\,\text{Sc}}\left(\frac{\partial^2\xi}{\partial X^2}+\frac{\partial^2\xi}{\partial Y^2}\right), \tag{4}$$

for the solid-material elements

$$\frac{1}{\text{Fo}_i}\frac{\partial\Theta_i}{\partial\tau}=\frac{\partial^2\Theta_i}{\partial X^2}+\frac{\partial^2\Theta_i}{\partial Y^2},\quad i=\overline{1,4}. \tag{5}$$

For the formulated problem (1)–(5), the initial conditions have the form

$$\Psi\,(X, Y, 0) = 0\,,\quad \Omega\,(X, Y, 0) = 0\,,\quad \Theta\,(X, Y, 0) = \xi\,(X, Y, 0) = 0\,,$$

we specify $\Theta = 1$ on the heat-release source throughout the process and $\xi = 1$ in the inlet and on the impurity source.

The boundary conditions:

(1) at the boundary $X = 0$, the conditions allowing for the heat exchange with the external medium by convection and radiation

$$\frac{\partial\Theta_i\,(X, Y, \tau)}{\partial X} = \mathrm{Bi}_i\Theta_i\,(X, Y, \tau) - \mathrm{Bi}_i\Theta_{\mathrm{e}} + Q_i \tag{6}$$

are realized for

$$Q_i = N_i\left[\left(\Theta_i\,(X, Y, \tau) + \frac{T_0}{T_{\mathrm{h.s}} - T_0}\right)^4 - \left(\frac{T_{\mathrm{e}}}{T_{\mathrm{h.s}} - T_0}\right)^4\right],$$

where $i = 1$, 3, 4, and 5 in accordance with Fig. 1.

(2) at the remaining external boundaries, we specify the heat-insulation conditions

$$\frac{\partial\Theta_i\,(X, Y, \tau)}{\partial X^k} = 0\,,$$

where $X^1 \equiv X$ and $X^2 \equiv Y$; $i = 1$, 2, 3, and 5.

(3) on all portions of the solution domain where we have the conjugation of materials with different thermophysical characteristics, A. V. Luikov's conditions of the fourth kind

$$\Theta_i = \Theta_j\,,\quad \frac{\partial\Theta_i}{\partial X^k} = \lambda_{j,i}\frac{\partial\Theta_j}{\partial X^k}\,,\quad i, j = \overline{1, 5}\,,\quad i \neq j\,,\quad k = 1, 2$$

are fulfilled.

(4) at entry into the cavity (8 in Fig. 1), for the energy equation, we consider the boundary conditions of the 3rd kind (6) for the stream function, vorticity, and concentration:

$$\Psi = Y - \frac{h}{L_x}\,,\quad \Omega = 0\,,\quad \xi = 1\,;$$

(5) at exit from the cavity (9 in Fig. 1), we have

$$\frac{\partial\Psi}{\partial X} = \frac{\partial\xi}{\partial X} = \frac{\partial\Omega}{\partial X} = \frac{\partial\Theta}{\partial X} = 0\,;$$

(6) at the boundaries of the solid material and the gas that are parallel to the coordinate axes $0X(0Y)$, except for the boundaries adjacent to the cross section $Y = H/L_x$, we have

$$\Psi = 0\,,\quad \frac{\partial\Psi}{\partial Y\,(\partial X)} = 0\,,\quad \frac{\partial\xi}{\partial Y\,(\partial X)} = 0\,,\quad \Theta_i = \Theta_5\,,\quad \frac{\partial\Theta_i}{\partial Y\,(\partial X)} = \lambda_{5,i}\frac{\partial\Theta_5}{\partial Y\,(\partial X)}\,,\quad i = 1, 2, 4\,;$$

(7) at the boundaries that are adjacent to the cross section $Y = H/L_x$ and are parallel to the coordinate axes $0X(0Y)$, we have

$$\Psi = \frac{H - h}{L_x}\,,\quad \frac{\partial\Psi}{\partial Y\,(\partial X)} = 0\,,\quad \frac{\partial\xi}{\partial Y\,(\partial X)} = 0\,,\quad \Theta_i = \Theta_5\,,\quad \frac{\partial\Theta_i}{\partial Y\,(\partial X)} = \lambda_{5,i}\frac{\partial\Theta_5}{\partial Y\,(\partial X)}\,,\quad i = 1, 3\,.$$

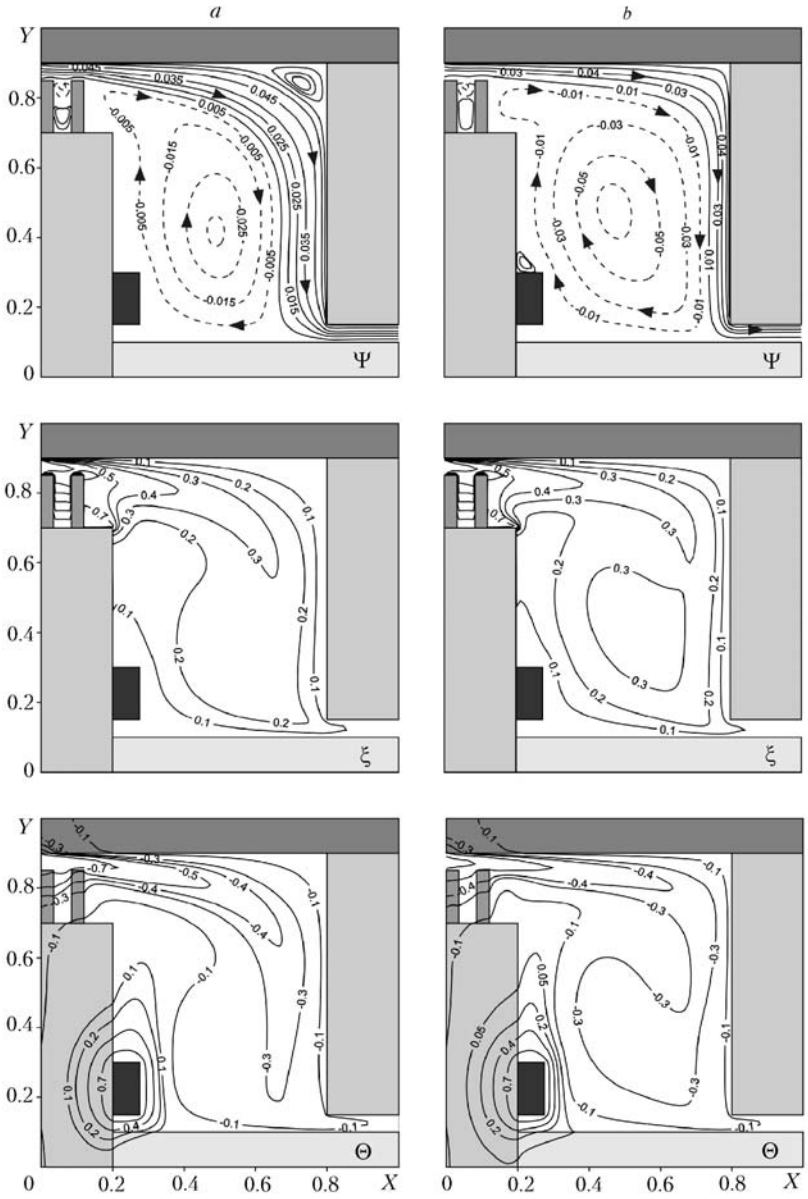

Fig. 2. Typical streamlines Ψ and fields of concentration ξ and temperature Θ at Re = 600, Br = 5, and τ = 100: a) Gr = 10^4 and b) 10^6.

Problem (1)–(5) with the corresponding boundary conditions is solved by the finite-difference method [16, 17]. The developed numerical algorithm is tested on model problems [18, 19]; the test results show satisfactory agreement with the works of other authors.

Discussion of Results. Numerical investigations of the boundary-value problem (1)–(5) have been carried out for the following values of the dimensionless numbers: $10^4 \le \mathrm{Gr} \le 10^7$, $10^2 \le \mathrm{Re} \le 10^3$, Pr = Sc = 0.7, and Br = −5, 1 and 5. The dimensionless governing temperatures and concentrations had the following values: $\Theta_e = -1$, $\Theta_{h.s} = 1$, $\Theta_0 = \xi_0 = 0$, and $\xi_{in} = \xi_{c.s} = 1$. The emphasis was on an analysis of the influence of the Gr and Re numbers characterizing respectively the strength of the heat-release source and the external forced flow (e.g., ventilation) and the parametric criterion Br describing the strength of the impurity source on the basic characteristics of the process under study.

Figure 2 shows the streamlines and the concentration and temperature fields corresponding to the regimes of mixed convection at Gr = 10^4 and 10^6. The arrows on the streamlines indicate the direction of gas motion.

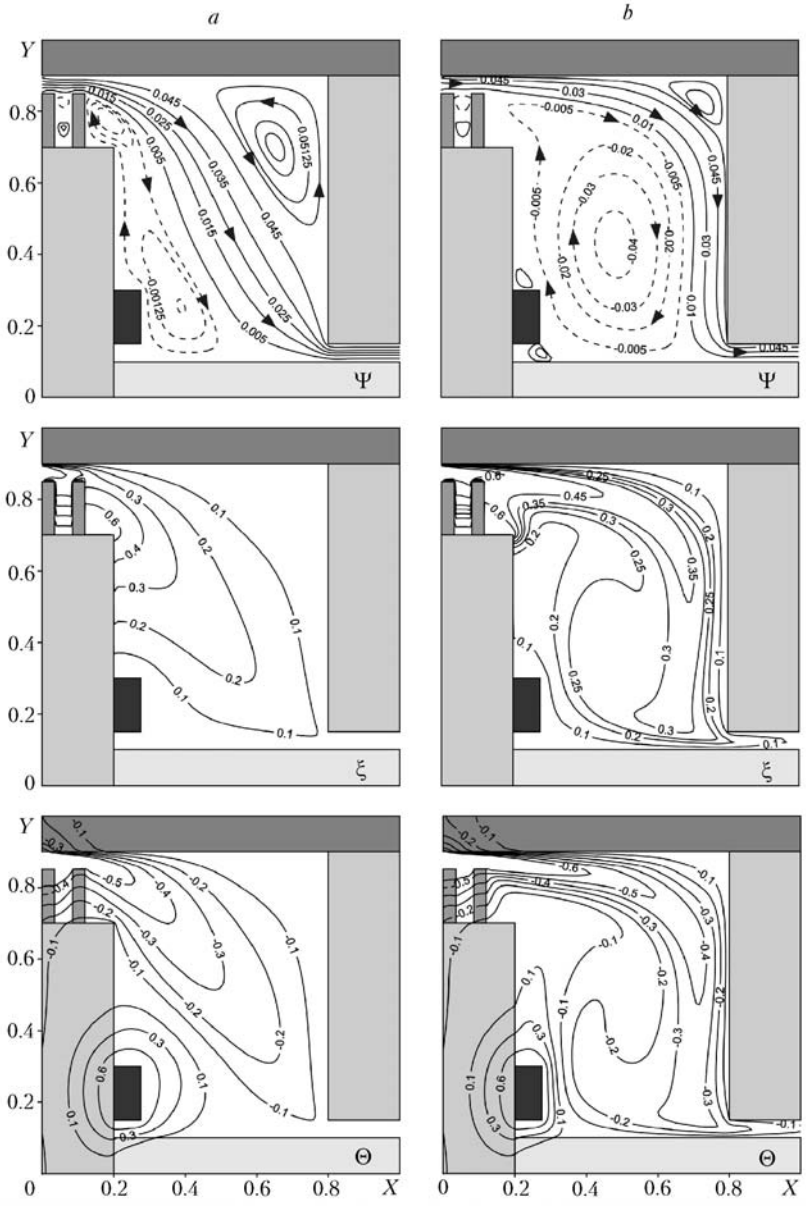

Fig. 3. Typical streamlines Ψ and fields of concentration ξ and temperature Θ at Gr = 10^4, Br = –5, and τ = 100: a) Re = 300 and b) 900.

When Gr = 10^4 (Fig. 2a) a single convective cell due to the influence of the heat-release source is formed in the gas cavity. This circulatory motion interacts with external forced flow to form secondary circulations in the corner zones of the gas cavity. Flows of rather low intensity are noticeable between the solid-material elements in the gas cell (4 in Fig. 1). The observed regime of flow leads to a nonuniform distribution of the impurity concentration in the cavity. The impurity penetrates deep into the cavity due to the forced flow on the source side of the external medium, but bends in the constant-concentration lines, which are caused by the presence of the convective cell, are seen. The temperature field in turn reflects the dominant influence of the external forced flow over the heat-release source. A substantial cooling of the gas cavity is observed. The elevated-temperature front is formed near the heat source and moves slightly forward in the vertical direction. The temperature in the solid-material elements at the boundary $X = 0$ changes, due mainly to the low environmental temperature. Since the regimes of convective heat transfer are characterized by the interaction of the flow field and the temperature field, the change in the contours of the constant-temperature lines, which is matched to the streamlines of the convective cell, is noticeable in the figure reflecting the isotherms.

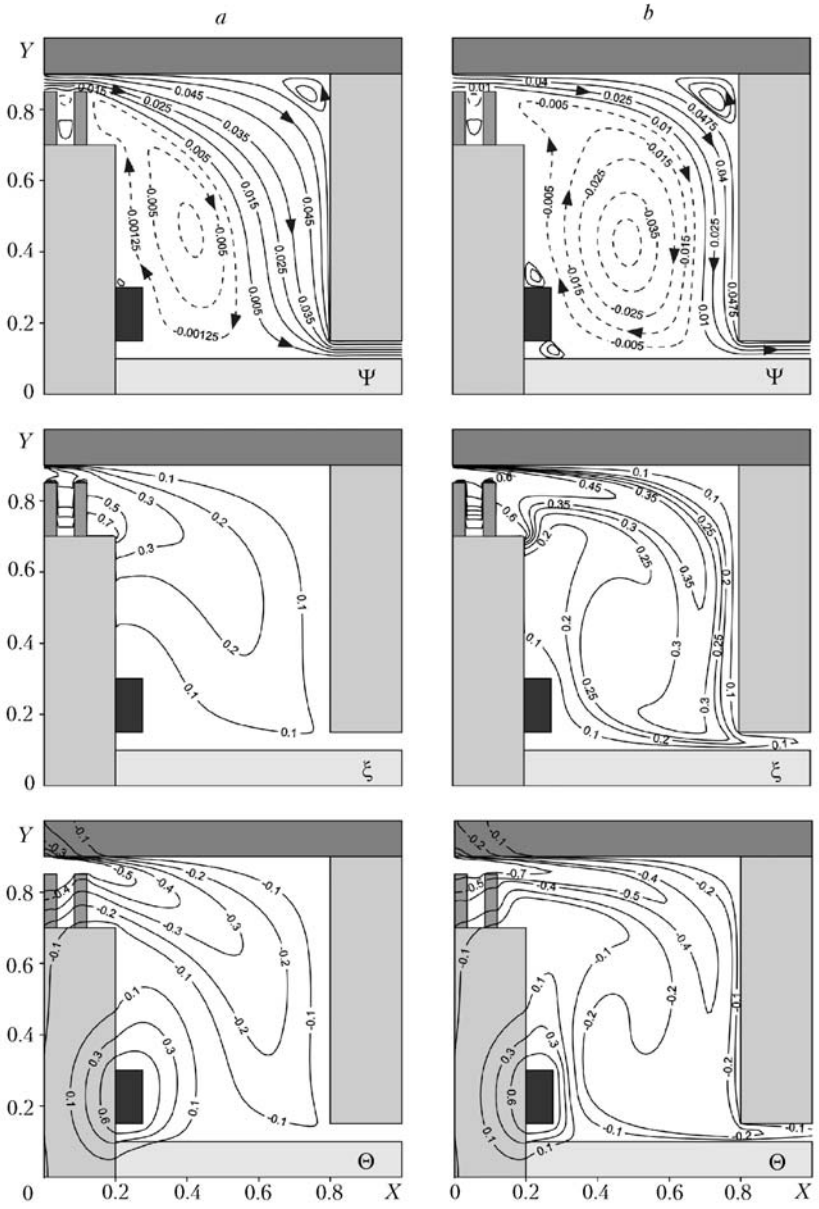

Fig. 4. Typical streamlines Ψ and fields of concentration ξ and temperature Θ at Gr = 10^4, Br = 1, and τ = 100: a) Re = 300 and b) 900.

An increase of 100 times in the Grashof number (Fig. 2b) causes the dimensions of the convective cell to grow. This has an effect on the peculiar choking of the forced flow at the upper wall, which leads to a dissipation of the secondary circulation in the right-hand upper corner of the gas cavity. The higher value of the lift has an effect on the growth in the gas velocities in the convective cell. The propagation of the influence of the lift up to the inlet is quite nontrivial, namely, in the gas interlayer of zone 4 (Fig. 1), we observe a change in the circulation scale due to the displacement of forced flow. The concentration field changes only slightly — the constant-concentration line corresponding to a value of 0.3 is divided, which is due to the higher velocities and the dimension of the convective cell. Modification of the temperature field is nontypical of this regime to a certain degree. It is assumed that increase in the Grashof number will lead to a more intense heating of the cavity but, e.g., the area that is enclosed by the isotherm corresponding to a value of the dimensionless temperature of –0.3 grows. Thus, the increased region of the convective cell has an effect on the internal cooling of the cavity but keeps the low-temperature front from moving forward. For example, isotherms corresponding to dimensionless temperatures of –0.4 and –0.5 enclose smaller areas than those in the regimes of low Grashof numbers (Fig. 2a).

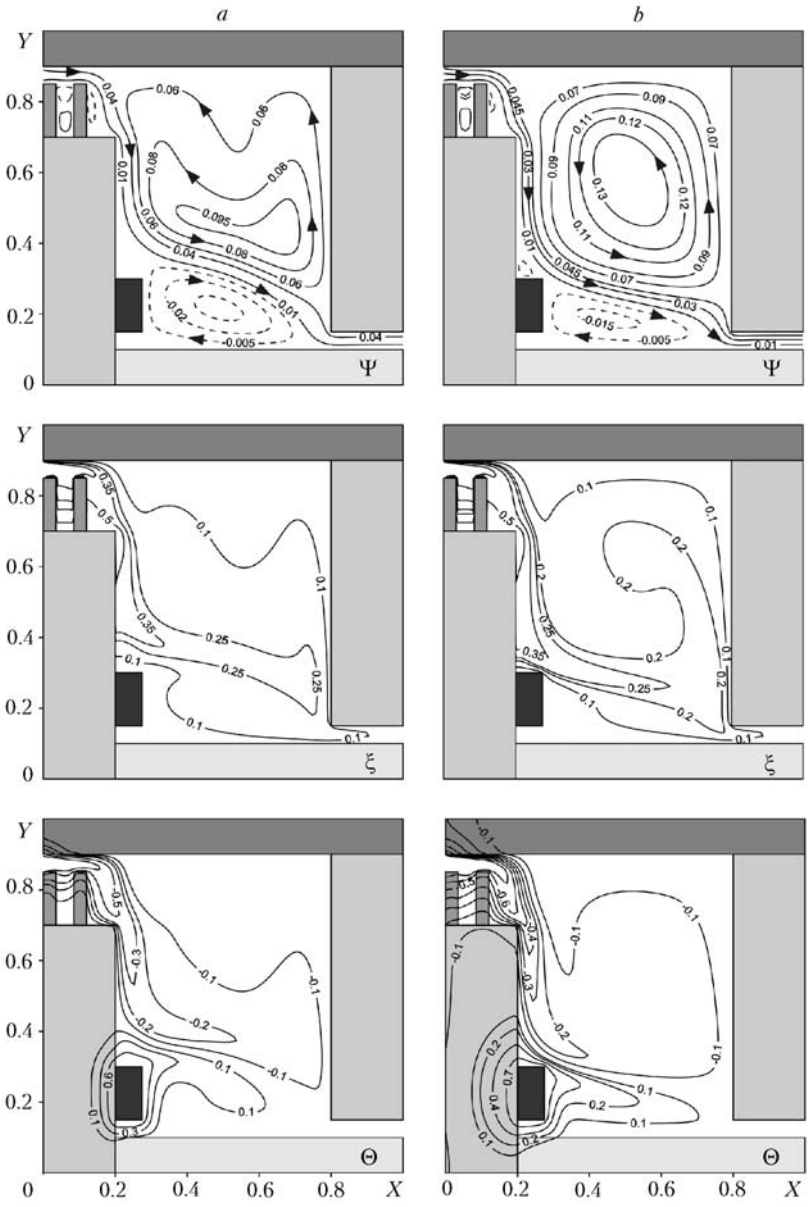

Fig. 5. Typical streamlines Ψ and fields of concentration ξ and temperature Θ at Re = 600, Br = −5, and Gr = 10^6: a) τ = 20 and b) 100.

The influence of the intensity of external forced flow on the distributions of the isotherms, the streamlines, and the constant-concentration lines has been analyzed (Fig. 3).

In the mixed-convection regime corresponding to Re = 300 and Gr = 10^4 (Fig. 3a), forced flow due to the small velocity of motion immediately behind the inlet "sinks" into the cavity, deforming the convective cell. The concentration field and the low-temperature field are completely determined by this external flow, and such a distribution can actually be predicted *a priori*. For the considered regime, we can decompose the processes of forced and natural convection on the indicated time interval, since they interact with each other only slightly.

Increase in the flow velocity at entry into the cavity produces significant changes in the thermohydrodynamic and diffusion fields (Fig. 3b).

The convective cell increases in dimension; a growth in the gas velocities in this vortex is noticeable, too. It should be noted that the increase in the circulation scale is related to the increase in the velocity at entry into the cavity, rather than to the growth in the lift, which is not so evident. The higher forced-flow intensity leads to a deformation of the secondary vortex in the right-hand upper corner of the gas cavity. The concentration field experiences

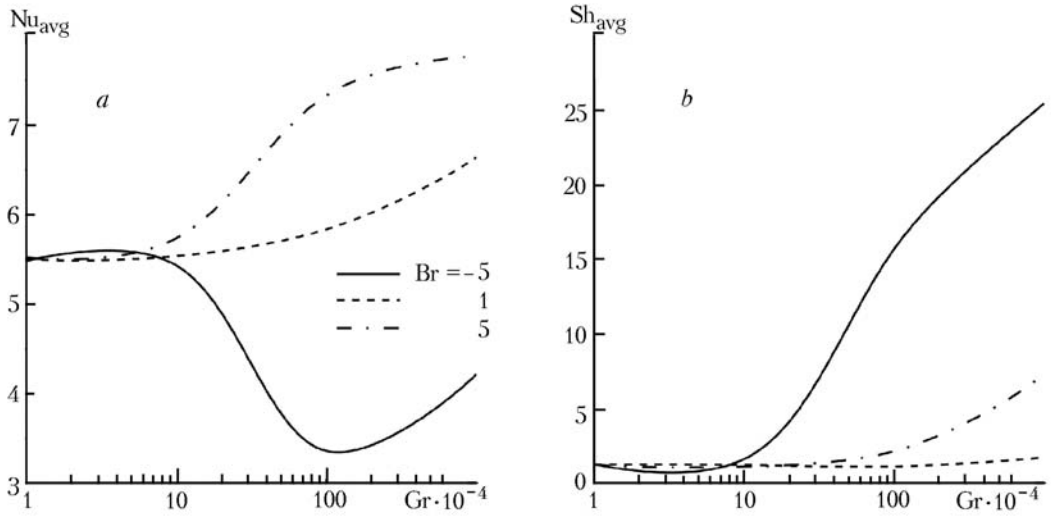

Fig. 6. Average Nusselt numbers (a) and average Sherwood number (b) vs. Grashof number and buoyancy parameter at Re = 900 and τ = 100.

changes: a more intense penetration of the impurity deep into the cavity occurs, but it is matched to the basic vortex now, i.e., here we observe a substantial relationship between mixed-convection mechanisms. The temperature field is nonuniform, too. A substantial cooling of the gas cavity is noticeable.

Change in the intensity of the mass-release source also has an effect on the distribution of the main parameters (Fig. 4). An increase in the buoyancy parameter to Br = 1 causes the dimensions of the convective cell to grow at Re = 300 and Gr = 10^4 (Fig. 4a). Also, we observe a change in the configuration of the constant-concentration lines in the zone of the left-hand wall due to the vortex in this region. The heat torch above the heat source does not "adjust" to the external forced flow but itself exerts an influence on this flow to a certain degree. The distributions of thermohydrodynamic and diffusion parameters in the regime Re = 900 and Gr = 10^4 (Fig. 4b) differ from the analogous distributions at Br = −5 only slightly.

The influence of the nonstationarity factor on the distributions of local basic characteristics has been analyzed. Figure 5 gives the streamlines and the concentration and temperature fields corresponding to the flow regime Re = 600, Br = −5, and Gr = 10^6 at different instants of time.

At τ = 20 (Fig. 5a), two convective cells having different dimensions and velocities of gas motion are formed in the gas cavity. Secondary flows appear in the gas interlayer of the solid-material elements (4 in Fig. 1). The vortex formed by the change in the direction of the external forced flow contains streamlines with nontypical bends, which is attributed to the initial step of formation of the flow field. The concentration is distributed rather nonuniformly: the impurity penetrates, due to the external forced flow, first to the heat source and then to the outlet. The position of the constant-concentration lines with values of ≥0.25 totally reflects the tube of forced flow. Owing to the external flow, the low-temperature front reaches the local heat-release source and deforms the heat torch, which changes orientation, reflecting the convective cell in the base zone.

An increase in the time interval to the instant τ = 100 (Fig. 5b) leads to a certain establishment of the circulation in the upper part of the cavity. Flow velocities increase in this vortex. This leads to a decrease in both the dimensions and the gas velocity in the convective cell due to the presence of the heat source. The concentration and temperature distribution is matched to the flow field. Heating of the solid-material element adjacent to the source and cooling of the wall on the source side of the X = 0 boundary by the external medium are noteworthy.

Also, we have analyzed the influence of the lift and the intensity of the mass-release source on the values of the average Nusselt and Sherwood numbers at the characteristic boundaries of the gas cavity and the solid-material elements:

$$\mathrm{Nu}_{\mathrm{avg}} = \frac{1}{0.75}\int_{0.15}^{0.9}\left|\frac{\partial\Theta}{\partial X}\right|_{X=0.8} dY \quad \text{and} \quad \mathrm{Sh}_{\mathrm{avg}} = \frac{1}{0.08}\int_{0.12}^{0.2}\left|\frac{\partial\xi}{\partial Y}\right|_{Y=0.7} dX .$$

Figure 6 plots the average Nusselt and Sherwood numbers as functions of the intensity of the heat and mass sources. It is clearly seen that the buoyancy parameter has a slight effect on the generalized heat- and mass-exchange coefficients when $\mathrm{Gr} \le 10^5$. Substantial changes in the values of the these coefficients are observed with further growth in the Grashof number. The average Nusselt number increases with buoyancy parameter Br, which is due to the intense cooling in the zone of the right-hand element of the solid material. The average Sherwood number acts nonmonotonically with variation in the parametric criterion Br, which characterizes the instability of the analyzed process, if not the substantial interrelation of the processes of transfer of heat and mass.

Conclusions. We have mathematically modeled mixed convection under mass-transfer conditions in the rectangular region with the walls of finite thickness in a fairly wide range of variation in the governing parameters $10^4 \le \mathrm{Gr}\ 10^7$, $10^2 \le \mathrm{Re} \le 10^3$, Pr = Sc = 0.7, and Br = –5, 1, and 5. The substantial influence of the internal mass transfer on both the local characteristics of the heat-transfer process and the structure of the integral heat- and mass-exchange coefficients has been shown. The scale of influence of the buoyancy force on the formation of certain flow regimes has been established. The role of the heat and impurity sources in the process of conjugate heat and mass transfer has been determined. The distinctive features of the streamline and temperature distributions, which correspond to different flow regimes, have been recognized. The influence of the nonstationarity factor which is caused not only by the thermal inertia of the solid-material elements but also by the formation, development, and dissipation of vortex structures due to the influence of the heat and mass sources has been shown. The plots of the average Nusselt and Sherwood numbers at the boundaries of the gas cavity and the solid wall in the investigated range of variation in the Grashof number and the parametric criterion have been obtained.

This work was carried out with financial support from the Russian Foundation for Basic Research (No. 08-08-00402-a).

NOTATION

a, thermal diffusivity, $\mathrm{m}^2/\mathrm{sec}$; $\mathrm{Bi}_i = \alpha L_x/\lambda_i$, Biot number corresponding to the ith material; $\mathrm{Br} = (\beta_c \Delta C)/(\beta \Delta T)$, parametric criterion (buoyancy parameter); C, concentration of the impurity in the solution domain; C_0, initial concentration of the impurity in the solution domain; $C_{\mathrm{s.c}}$, concentration of the impurity on the mass source; C_{in}, concentration of the impurity at entry into the cavity; D, diffusion coefficient, $\mathrm{m}^2/\mathrm{sec}$; $\mathrm{Fo}_i = a_i t_0/L_x^2$, Fourier number corresponding to the ith material; $\mathrm{Gr} = \beta g_y L_x^3 (T_{\mathrm{h.s}} - T_0)/\nu^2$, Grashof number; $\mathbf{g}$, gravitational vector; g_y, component of gravitational acceleration in the projection onto the y axis ($g_x = 0$), $\mathrm{m}/\mathrm{sec}^2$; H, distance between the cross section $y = 0$ and the lower boundary of the upper wall; h, distance between the cross section $y = 0$ and the upper boundary of the solid-material elements (4 in Fig. 1); L_x, dimension of the solution domain along the x axis, m; L_y, dimension of the solution domain along the y axis, m; $\mathrm{N}_i = \varepsilon\sigma L_x (T_{\mathrm{h.s}} - T_0)^3/\lambda_i$, Stark number corresponding to the ith material; $\mathrm{Nu}_{\mathrm{avg}}$, average Nusselt number at the boundary $X = 0.8$, $0.15 \le Y \le 0.9$; $\mathrm{Pr} = \nu/a$, Prandtl number; Q_i, dimensionless heat flux determining the role of conduction and radiation at the boundary of the ith material; $\mathrm{Re} = V_{\mathrm{in}} L_x/\nu$, Reynolds number; $\mathrm{Sc} = \nu/D$, Schmidt number; $\mathrm{Sh}_{\mathrm{avg}}$, average Sherwood number at the boundary $Y = 0.7$, $0.12 \le H \le 0.2$; T, temperature, K; T_0, initial temperature of the solution domain, K; T_{e}, environmental temperature, K; $T_{\mathrm{h.s}}$, temperature on the heat-release source, K; t, time, sec; t_0, time scale, sec; U and V, dimensionless velocity components corresponding to u and v; V_{in}, velocity scale (flow velocity at entry into the cavity), m/sec; u and v, velocity components in the projection onto the x and y axes respectively, m/sec; X^k, kth unit vector of the coordinate system; x, y, Cartesian coordinates; α, coefficient of heat exchange between the external medium and the solution domain in question, $\mathrm{W}/(\mathrm{m}^2 \cdot \mathrm{K})$; β, temperature coefficient of volumetric expansion, K^{-1}; $\beta_C = -(\partial\rho/\partial C)_{p,T}/\rho$, diffusion coefficient of volumetric expansion; ε, reduced emissivity; Θ, dimensionless temperature; Θ_0, initial dimensionless temperature of the solution domain; Θ_{e}, dimensionless environmental temperature; $\Theta_{\mathrm{h.s}}$, dimensionless temperature on the heat-release source; Θ_i, dimensionless temperature of the ith material; λ_i, thermal conductivity of the ith material, $\mathrm{W}/(\mathrm{m} \cdot \mathrm{K})$; $\lambda_{j,i} = \lambda_j/\lambda_i$, relative thermal conductivity; ν, coefficient of kinematic viscosity, $\mathrm{m}^2/\mathrm{sec}$; ξ, dimensionless concentration of the impurity; ξ_0, initial dimensionless concentration of the impurity in the solution domain; $\xi_{\mathrm{c.s}}$, dimensionless concentration of the impurity on the mass source; ξ_{in}, dimensionless concentration of the impurity at entry in the cavity; σ, Stefan–Boltzmann constant, $\mathrm{W}/(\mathrm{m}^2 \cdot \mathrm{K}^4)$; τ, dimensionless time; Ψ, dimensionless stream function corresponding to ψ; ψ, stream function in $u = \partial\psi/\partial y$ and $v = -\partial\psi/\partial x$, $\mathrm{m}^2/\mathrm{sec}$; $\psi_0 = V_{\mathrm{in}} L_x$, vorticity-vector scale, $\mathrm{m}^2/\mathrm{sec}$; Ω, dimensionless

analog of the vorticity-vector, corresponding to ω; ω, vorticity of velocity $\omega = \partial v/\partial x - \partial u/\partial y$, 1/sec; $\omega_0 = V_{in}L_x$, vortex-vector scale, 1/sec. Subscripts and superscripts: 0, initial instant of time; avg, average value; *C*, corresponds to the concentration field; c.s, impurity source; e, environment; h.s, heat source; in, zone of entry into the cavity; *i* and *j*, material number; *k*, ordinal number of the unit vector of the coordinate system.

REFERENCES

1. Qi-Hong Deng and Guoqiang Zhang, Indoor air environment: more structures to see? *Building Environment*, **39**, 1417–1425 (2004).
2. Marcelo J. S. de Lemos and Luzia A. Tofaneli, Modeling of double-diffusive turbulent natural convection in porous media, *Int. J. Heat Mass Transfer*, **47**, 4233–4241 (2004).
3. E. Papanicolaou and V. Belessiotis, Double-diffusive natural convection in an asymmetric trapezoidal enclosure: unsteady behavior in the laminar and the turbulent-flow regime, *Int. J. Heat Mass Transfer*, **48**, 191–209 (2005).
4. Fu-Yun Zhao, Di Liu and Guang-Fa Tang, Natural convection in an enclosure with localized heating and salting from below, *Int. J. Heat Mass Transfer*, **51**, 2889–2904 (2008).
5. D. Liu, F. Y. Zhao, and G. F. Tang, Thermosolutal convection in a saturated porous enclosure with concentrated energy and solute sources, *Energy Conservation Management*, **49**, 16–31 (2008).
6. Y. Jaluria, *Natural Convection: Heat and Mass Transfer* [Russian translation], Mir, Moscow (1983).
7. Yu. A. Sokovishin and O. G. Martynenko, *Introduction to the Theory of Free-Convective Heat Transfer* [in Russian], Izd. LGU, Leningrad (1982).
8. B. Gebhart, Y. Jaluria, R. L. Mahajan, and B. Sammaki, *Buoyancy-Induced Flows and Transport* [Russian translation], Vol. 1, Mir, Moscow (1991).
9. A. Liaqat and A. C. Baytas, Conjugate natural convection in a square enclosure containing volumetric sources, *Int. J. Heat Mass Transfer*, **44**, 3273–3280 (2001).
10. A. A. Merrikh and J. L. Lage, Natural convection in an enclosure with disconnected and conducting solid blocks, *Int. J. Heat Mass Transfer*, **48**, 1361–1372 (2005).
11. A. Bejan, *Convection Heat Transfer*, Wiley, New York (2004).
12. Qi-Hong Deng, Jiemin Zhou, Chi Mei, and Yong-Ming Shen, Fluid, heat and contaminant transport structures of laminar double-diffusive mixed convection in a two-dimensional ventilated enclosure, *Int. J. Heat Mass Transfer*, **47**, 5257–5269 (2004).
13. A. Muftuoglu and E. Bilgen, Conjugate heat transfer in open cavities with a discrete heater at its optimized position, *Int. J. Heat Mass Transfer*, **51**, 779–788 (2008).
14. E. Bilgen and A. Balkaya, Natural convection on discrete heaters in a square enclosure with ventilation ports, *Int. J. Heat Fluid Flow*, 29, 1182–1189 (2008).
15. A. V. Luikov, *Heat Conduction Theory* [in Russian], Vysshaya Shkola, Moscow (1967).
16. V. M. Paskonov, V. I. Polezhaev, and L. A. Chudova, *Numerical Simulation of Heat- and Mass-Transfer Processes* [in Russian], Nauka, Moscow (1984).
17. P. J. Roache, *Computational Fluid Dynamics* [Russian translation], Mir, Moscow (1980).
18. B. Calcagni, F. Marsili, and M. Paroncini, Natural convective heat transfer in square enclosures heated from below, *Appl. Thermal Eng.*, **25**, 2522–2531 (2005).
19. D. A. Kaminski and C. Prakash, Conjugate natural convection in a square enclosure: effect of conduction on one of the vertical walls, *Int. J. Heat Mass Transfer*, **29**, 1979–1988 (1986).